engineering proceedings

Proceeding Paper

Design of Highly Birefringence and Nonlinear Modified Honeycomb Lattice Photonic Crystal Fiber (MHL-PCF) for Broadband Dispersion Compensation in E+S+C+L Communication Bands †

Amit Halder [1,2,*], Md. Riyad Tanshen [1], Mst. Sumi Akter [1] and Mir Afzal Hossain [1]

1 Department of Electrical and Electronic Engineering, World University of Bangladesh, Uttara, Dhaka 1230, Bangladesh; riyadrt@gmail.com (M.R.T.); sumi.akter@eee.wub.edu.bd (M.S.A.); mh0810744@gmail.com (M.A.H.)
2 Department of Electrical and Electronic Engineering, Rajshahi University of Engineering and Technology, Kazla, Rajshahi 6204, Bangladesh
* Correspondence: amit.rueten@gmail.com

† Presented at the 4th International Electronic Conference on Applied Sciences, 27 October–10 November 2023; Available online: https://asec2023.sciforum.net/.

Abstract: This paper investigates the design and tuning of a Broadband Dispersion Compensating Modified Honeycomb Lattice Photonic Crystal Fiber (MHL-PCF) with outstanding features such as strong birefringence and nonlinearity. The proposed PCF for y polarization exhibits a negative dispersion coefficient of −263.9 ps/(nm·km) at 1.55 µm operating frequency and a high negative dispersion of −652.9 ps/(nm·km) when air-filled fraction (d_c/Λ) grows from 0.35 to 0.65. Because it is a polarization-maintaining fiber, it also exhibits birefringence. At 1.55 µm operating frequency, the suggested fiber exhibits 1.482×10^{-2} birefringence. The suggested MHL-PCF has a high nonlinear coefficient of 34.68 $W^{-1}km^{-1}$ at the same operating frequency. Numerical aperture is also investigated for MHL-PCF as it influences their light-guiding capabilities, light-coupling efficiency, mode control, dispersion qualities, and sensitivity in sensing applications. The numerical aperture of the proposed MHL-PCF at 1550 nm is 0.4175, demonstrating excellent light-coupling properties. The purpose of this research is to satisfy the growing need for improved optical communication systems capable of managing high data rates across long transmission distances. The suggested MHL-PCF structure has distinct features that make it an attractive choice for dispersion correction and nonlinear optical applications.

Keywords: Broadband Dispersion Compensating; Honeycomb Lattice Photonic Crystal Fiber; birefringence; nonlinearity; numerical aperture; optical communication systems

Citation: Halder, A.; Tanshen, M.R.; Akter, M.S.; Hossain, M.A. Design of Highly Birefringence and Nonlinear Modified Honeycomb Lattice Photonic Crystal Fiber (MHL-PCF) for Broadband Dispersion Compensation in E+S+C+L Communication Bands. *Eng. Proc.* **2023**, *56*, 19. https://doi.org/10.3390/ASEC2023-15234

Academic Editor: Andrea Ballo

Published: 26 October 2023

1. Introduction

Due to the fast expansion of optical communication networks, the creation of new optical fibers capable of solving the problems given by increased data rates and longer transmission lengths has become necessary [1]. Dispersion, a phenomenon in which various wavelengths of light move at different rates, is a substantial barrier to high-quality signal transmission. As data rates increase, dispersion control becomes increasingly important in order to preserve signal integrity and avoid data loss [2]. Photonic Crystal Fibers (PCFs) have emerged as a possible solution to dispersion-related difficulties due to their unique structural features and configurable guiding mechanisms. The notion of using photonic crystals for light steering was presented in the late twentieth century, ushering in a new age of optical fiber architecture [3]. Photonic crystals are periodic formations with refractive index changes that generate bandgaps, preventing certain wavelengths from propagating while allowing others to pass through. This intrinsic control over light propagation characteristics enables the development of fibers with specific dispersion qualities [4]. In recent years, the emphasis has switched toward producing PCFs with improved birefringence and nonlinearity for dispersion correction and nonlinear optical applications [5]. Birefringence, or the difference in refractive indices experienced by orthogonal polarizations, has attracted interest for its potential in polarization-maintaining fibers and polarization-dependent electronics. This characteristic enables precise control over polarization states, which is critical for signal integrity in polarization-sensitive systems [6]. Nonlinearity, another important feature in current optical fiber design, is caused by the Kerr effect, which is the change in refractive index caused by light intensity. High nonlinearity is desired for wavelength conversion, signal regeneration, and optical switching [7]. Furthermore, the capacity to build photonic crystal structures has opened up possibilities for modifying other critical parameters such as numerical aperture (NA). NA influences light-coupling efficiency, light-guiding capabilities, and sensitivity in sensing applications, hence it is critical in maximizing total fiber performance [8]. A single-mode hybrid cladding circular photonic crystal fiber (HyC-CPCF) with strong birefringence (2.1×10^{-2}) and a significant negative dispersion coefficient (-650 ps/(nm·km)) at 1550 nm wavelength is introduced by Haque et al. (2015) [9]. The construction is more complicated since it comprises many elliptical air holes with erratic patterns. In order to attain a considerable negative dispersion coefficient (varying from -242.22 to -762.6 ps/(nm·km)) and ultra-high birefringence (2.64×10^{-2}) over a broad wavelength range (1.30 to 1.65 μm), Hasan et al. propose a single-mode photonic crystal fiber (PCF) using a hybrid cladding design [10]. The potential of this dispersion-compensating PCF is illustrated by the study's thorough discussion of a variety of fiber metrics, including residual dispersion, effective dispersion, effective area, confinement loss, and nonlinear coefficient. A distinct hybrid cladding photonic crystal fiber (PCF) with birefringence of 1.46×10^{-2} and decreased negative dispersion of -274.5 ps/(nm·km) is presented by Prabu and Malavika (2019), demonstrating its potential for use in sensing and communications [11]. A photonic crystal fiber (PCF) with air-hole flaws built into a hybrid fiber core was introduced by G. D. Krishna et al. In an equilateral triangle configuration, the core has three equal air holes. With a reasonably low confinement loss of 9.51×10^{-2} decibels per meter (dB/m), this design intends to achieve a negative dispersion of -11.63 (ps/(nm·km)) [12]. Halder and Anower propose an optimized design for a highly birefringent hybrid photonic crystal fiber (Hy-PCF) capable of broadband compensation across the S, C, and L communication bands (1400 nm to 1625 nm). Their study demonstrates a high birefringence of 3.039×10^{-2} and a significant nonlinear coefficient (33.76 W^{-1} km^{-1}) at 1550 nm wavelength while exhibiting dispersion compensation properties across a broad wavelength range. The proposed Hy-PCF design features a negative dispersion coefficient of -378.6 ps/(nm·km) at 1550 nm, along with a relative dispersion slope closely resembling that of a single-mode fiber [13]. Halder (2020) presents a slope-matched hybrid dispersion compensating fiber design with significant birefringence (3.76×10^{-2}) and an effective dispersion compensation range (1400–1625 nm), achieving a dispersion coefficient of -606 ps/(nm·km) at 1550 nm. This design showcases the potential for high bit-rate communication and sensing applications, along with low confinement loss (3.756×10^{-10} dB/m) [14].

This paper presents a comprehensive investigation into the design and tuning of a Modified Honeycomb Lattice Photonic Crystal Fiber (MHL-PCF) with exceptional features. By exploiting the unique properties of the honeycomb lattice structure, the proposed fiber achieves strong birefringence of 1.482×10^{-2}, a high nonlinear coefficient of 34.68 $W^{-1}km^{-1}$, and broadband dispersion compensation (-652.9 ps/(nm·km) at 1550 nm operating wavelength). The negative dispersion coefficient and significant tunability of the fiber's dispersion characteristics hold promise for effectively managing dispersion across a wide range of operating conditions. Furthermore, the high numerical aperture underscores the fiber's potential for efficient light coupling and versatile applications.

2. Geometry of the Proposed MHL-PCF

The transverse sectional view of the proposed Modified Honeycomb Lattice Photonic Crystal Fiber (MHL-PCF) in Figure 1 showcases a well-distributed arrangement of circular air holes. The design intentionally avoids the use of non-circular air holes, such as rectangles or ellipses, to maintain a simple fabrication process. The MHL-PCF structure consists of eight layers of air-hole rings making a honeycomb lattice structure, all circular in shape, and utilizes fused silica as the background material. The initial layer of the air hole ring consists of six air holes, four of which have diameters of $d_c = 0.45\ \Lambda = 0.36\ \mu m$ and the other two of which have diameters of $d_1 = d = 0.9\ \Lambda = 0.72\ \mu m$ with a pitch of $\Lambda = 0.8\ \mu m$. The other air hole rings are the same size as d, therefore $d_2 = d_3 = d_4 = d_5 = d_6 = d_7 = d_8 = d = 0.72\ \mu m$. The ratio d_c/Λ was varied and examined to investigate the influence of air filling fraction on dispersion and birefringence. The pitch (Λ) was also changed to see how the dispersion and birefringence qualities changed. To produce and create photonic crystal fibers, various key manufacturing procedures such as sol-gel casting [15], traditional drilling [16], stack and draw method [17], and so on are used. Because the design comprises uniform air holes, it is simple to construct using the stack-and-draw approach. The introduction of nanotechnology has also facilitated the manufacture of the smallest of structures.

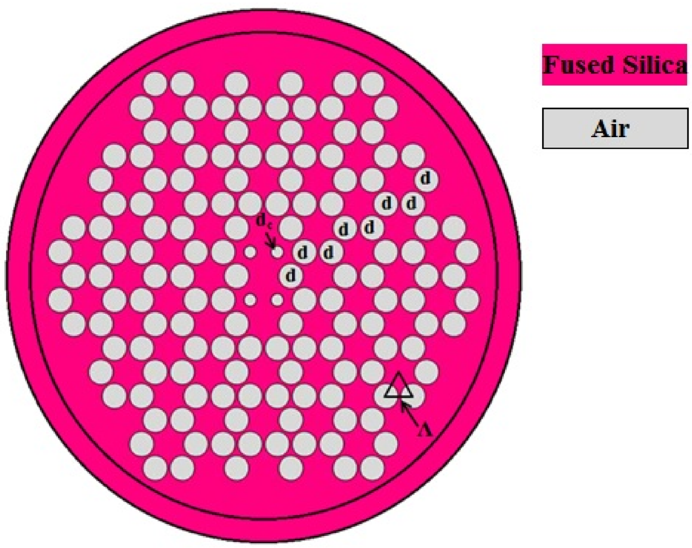

Figure 1. Proposed Modified Honeycomb Lattice Photonic Crystal Fiber (MHL-PCF) in cross-sectional view. Where, pitch, $\Lambda = 0.8\ \mu m$, $d_c/\Lambda = 0.45$ and $d/\Lambda = 0.9$.

3. Simulation Techniques and Computational Methods

The investigation into the guiding properties of the MHL-PCF involved numerical simulations. Given the microstructural nature of the proposed PCF, electromagnetic analysis, encompassing field distribution and effective mode indices, was conducted using the finite element method (FEM) [18]. To perform these analyses, COMSOL Multiphysics version 4.2, a commercially available FEM-based software tool, was employed [19]. To mitigate issues related to reflection and backscattering, a circular perfectly matched layer (PML) with a thickness corresponding to 10% of the cladding radius was implemented along the periphery of the designed structure [20]. This PML layer ensured the effective absorption of unwanted reflections. The PML thickness consistently applied around the MHL-PCF was set at 1 μm, with a scaling factor of 1. A refined meshing technique was adopted for accurate representation. Within this framework, the finite element method computed the propagation constant β by employing mode analysis, solving Maxwell's equations within the microstructure design. The refractive index $n(\lambda)$ of the substrate material, silica, was considered wavelength-dependent and computed using the Sellmeier equation [21], which takes the form:

$$n(\lambda) = \sqrt{(1 + \sum_{i=1}^{N} \frac{B_i \lambda^2}{\lambda^2 - C_i})} \quad (1)$$

Here, n(λ) stands for the wavelength-dependent refractive index of the material, λ denotes the wavelength in μm, and B_i and C_i represent empirically determined Sellmeier coefficients for the material. In most cases, the refractive index for glass is approximately 3. With the propagation constant β determined, the effective refractive index n_{eff} was subsequently computed using the following formula [22].

$$n_{eff} = \frac{\beta(\lambda, n(\lambda))}{k_0} \quad (2)$$

where λ_0 represents $2\pi/\kappa_0$, with κ_0 being the wave number of free space, and n_{eff} is the effective refractive index that is not only influenced by the wavelength but also varies with the specific mode. This characteristic renders it the term "modal index." In this section, the formulations for different optical parameters that govern the guiding properties of the photonic crystal fiber (PCF) are delved into. These parameters include dispersion, modal birefringence, numerical aperture, non-linearity, and confinement loss. The wavelength-dependent chromatic dispersion D(λ) of the PCF is derived from the effective refractive index n_{eff} of the fundamental mode, as outlined by the following expression [23].

$$D(\lambda) = -(\frac{\lambda}{c})(\frac{d^2 \mathrm{Re}[n_{eff}]}{d\lambda^2}) \quad (3)$$

The unit of dispersion is expressed as picoseconds per nanometer per kilometer (ps/(nm.km)), where λ represents the wavelength in micrometers (μm), c is the velocity of light in a vacuum, and n(λ) signifies the real part of the modal refractive index for a given wavelength λ. The chromatic dispersion of the photonic crystal fiber (PCF) can be controlled by manipulating its geometrical parameters such as pitch Λ, diameter d, and arrangement of air holes within the PCF structure. The modal birefringence B depends on the polarization-dependent effective refractive indices and is calculated using the equation outlined in reference [24].

$$B = \left| n_{eff,x} - n_{eff,y} \right| \quad (4)$$

where $\boldsymbol{n_{eff,x}}$ and $\boldsymbol{n_{eff,y}}$ represent the effective refractive indices of the two orthogonal polarization modes: x-polarization and y-polarization, respectively. However, the PCF's non-linearity is significantly influenced by the core's optical parameters, particularly the effective mode area A_{eff}. The core's effective area A_{eff} is determined as per the following definition provided in reference [25]:

$$A_{eff} = \frac{\left(\iint \left|\vec{E}\right|_2 dxdy\right)^2}{\iint \left|\vec{E}\right|_4 dxdy} \quad (5)$$

The effective mode area is quantified in square micrometers (μm^2), and **E** signifies the electric field. The non-linearity, denoted as γ, exhibits an inverse relationship with the effective mode area A_{eff}, as stated in reference. This characteristic can be succinctly expressed using the subsequent definition [26]:

$$\gamma = \left(\frac{2\pi}{\lambda}\right) \times \left(\frac{n_2}{A_{eff}}\right) \quad (6)$$

The non-linearity is measured in $W^{-1}km^{-1}$, and n_2 represents the Kerr constant of the material, expressed in square meters per watt (m^2/W).

In photonic crystal fibers (PCFs), the optical power is predominantly confined within the core region due to the higher refractive index in comparison to the lower refractive index of the surrounding cladding, which comprises air holes. Nonetheless, owing to the finite arrangement of air holes adjacent to the core, a portion of optical energy inevitably extends into the cladding area, resulting in what is known as confinement loss or leakage loss. This phenomenon is quantified by the term confinement loss L_c, which can be calculated using the subsequent equation [27]:

$$L_c = 8.686 \times k_0 \times \text{Im}[n_{eff}] \tag{7}$$

The confinement loss is measured in decibels per meter (dB/m), and Im[n_{eff}] represents the imaginary part of the effective refractive index for a specific mode.

The extent of optical power gathering within a photonic crystal fiber (PCF) is evaluated through the numerical aperture NA, a dimensionless factor. The mathematical representation of the numerical aperture (NA) can be expressed as follows [28]:

$$NA = \left[1 + \frac{\pi A_{eff}}{\lambda^2}\right]^{-0.5} \tag{8}$$

4. Numerical Results and Discussion

The section has extensively examined the optical characteristics relevant to communication frequencies. The focal range for communication wavelengths is 1280 nm to 1790 nm, encompassing the E, S, C, and L communication bands. From Figure 2, it can be observed that the chromatic dispersion for x-polarization is −167.4 ps/(nm·km), and for y-polarization is −263.9 ps/(nm·km) at the operating frequency of 1550 nm. The plot shows a negative dispersion slope, indicating the fiber's capability to compensate for dispersion over a wide range of wavelengths in both x and y polarizations.

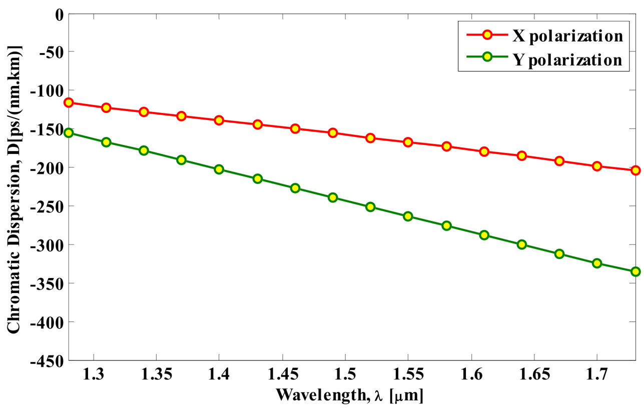

Figure 2. The dispersion curves of the proposed MHL-PCF for X and Y polarizations as a function of wavelength.

Figure 3a illustrates the dispersion properties of the Modified Honeycomb Lattice Photonic Crystal Fiber (MHL-PCF) for X polarization at different pitch values. As the pitch value increases from 0.8 to 1 micrometer, the dispersion decreases from −167.4 to −85.4 ps/(nm·km), indicating improved dispersion compensation capabilities. However, at a pitch of 0.9 μm, the dispersion increases slightly to −119.3 ps/(nm·km), suggesting an optimal pitch value for optimal dispersion compensation. In Figure 3b the dispersion coefficients are −263.9 ps/(nm·km) for a pitch of 0.8 μm, −171.1 ps/(nm·km) for a pitch of 0.9 μm, and −110 ps/(nm·km) for a pitch of 1 micrometer. The plot highlights how altering the pitch value affects the dispersion characteristics for Y polarization.

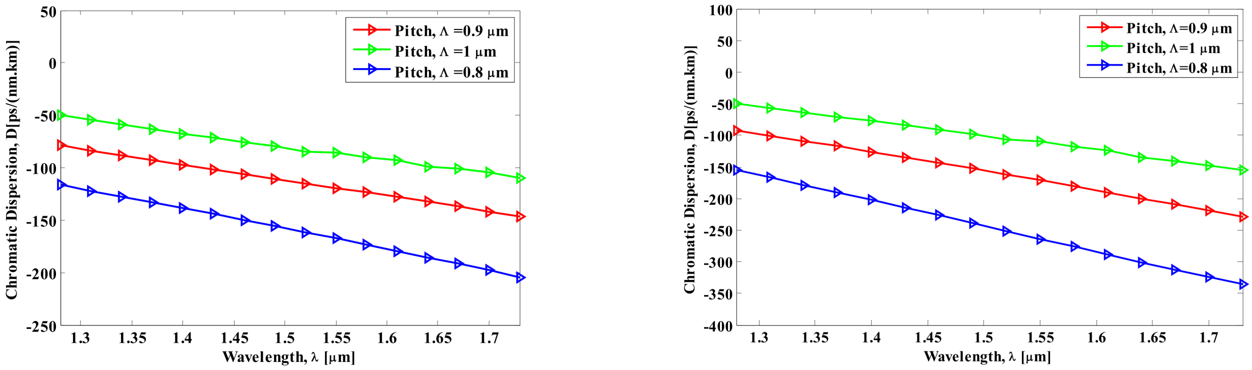

(**a**) (**b**)

Figure 3. Chromatic Dispersion vs. wavelength for (**a**) X polarization and (**b**) Y polarization with different pitch (Λ) values.

Figure 4 displays the variations of chromatic dispersion with wavelength for (a) X polarization and (b) Y polarization in the proposed Modified Honeycomb Lattice Photonic Crystal Fiber (MHL-PCF). The dispersion characteristics are obtained by adjusting the air-filled fraction by varying the ratio of air-hole diameter (d_c) to the lattice constant (Λ). For X polarization, the dispersion is negative, ranging from −92.62 ps/(nm·km) to −440.3 ps/(nm·km), as d_c/Λ increases from 0.35 to 0.65. Similarly, for Y polarization, the dispersion is also negative, varying from −156.7 ps/(nm·km) to −652.9 ps/(nm·km) as d_c/Λ increases from 0.35 to 0.65, showcasing the tunability of chromatic dispersion in the MHL-PCF for different polarizations.

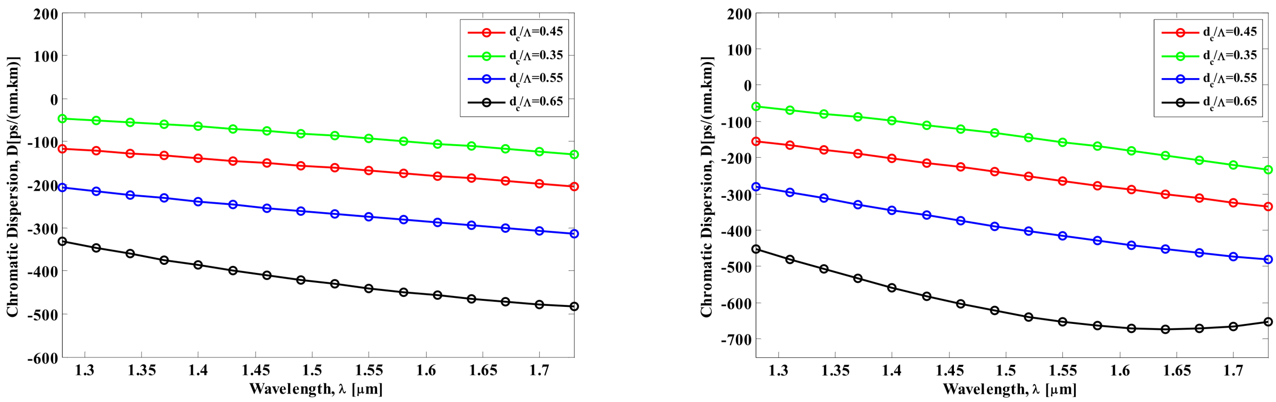

(**a**) (**b**)

Figure 4. The variations of chromatic dispersion with wavelength for (**a**) X polarization and (**b**) Y polarization, achieved by constant (Λ = 0.8μm). Varying the ratio of air-hole diameter (d_c) to the lattice.

Figure 5 presents the wavelength versus birefringence graphs for (a) different pitch (Λ) values and (b) different air-hole diameter (d_c) to lattice constant (Λ) ratios (d_c/Λ) at a fixed Λ of 0.8 μm. In Figure 5a, as the pitch increases from 0.8 μm to 1 μm, the birefringence decreases from 1.482×10^{-2} to 1.113×10^{-2}. In Figure 5b, varying dc/Λ from 0.35 to 0.65 leads to birefringence changes from 1.379×10^{-2} to 1.337×10^{-2}. Meanwhile, there is an increase in birefringence (1.499×10^{-2}) for $d_c/\Lambda = 0.55$ is recorded. The optimum birefringence of 1.482×10^{-2} was observed for $d_c/\Lambda = 0.45$ and Λ = 0.8 μm at 1550 nm operating wavelength. These results demonstrate how adjusting pitch and d_c/Λ influences the birefringence properties of the Modified Honeycomb Lattice Photonic Crystal Fiber (MHL-PCF) for potential polarization-sensitive applications.

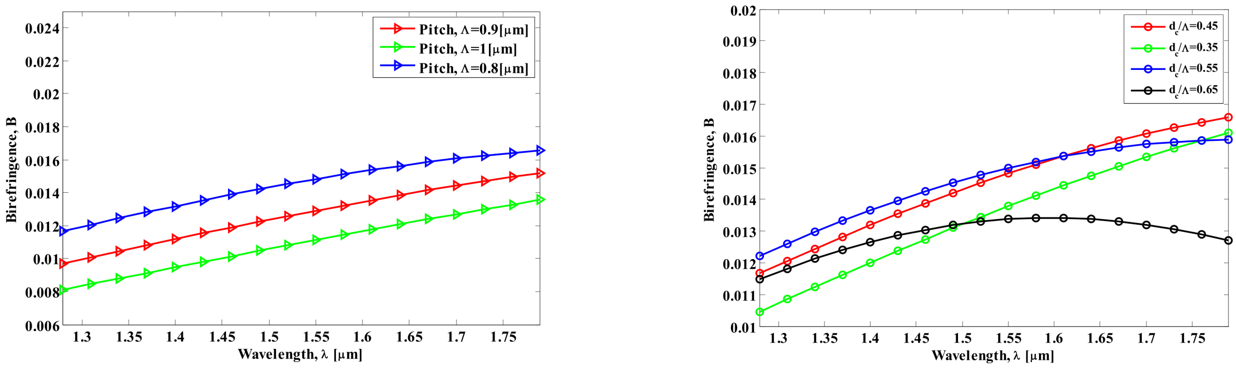

(**a**) (**b**)

Figure 5. Wavelength versus Birefringence graph (**a**) by varying different pitch (Λ) values and (**b**) by varying d_c/Λ values where Λ = 0.8 μm.

Figure 6 examines the nonlinearity and effective area of the proposed MHL-PCF. The suggested PCF structure's nonlinear coefficient at 1.55 μm wavelength is 34.68 W^{-1} km^{-1}, which is deemed strong nonlinearity in nature. At the same operating wavelength, the effective area of the proposed PCF is found to be 3.623 μm^2. Because of the decreased effective area, the PCF is a possibility for significant nonlinear effects, which also makes it a supercontinuum generator [29].

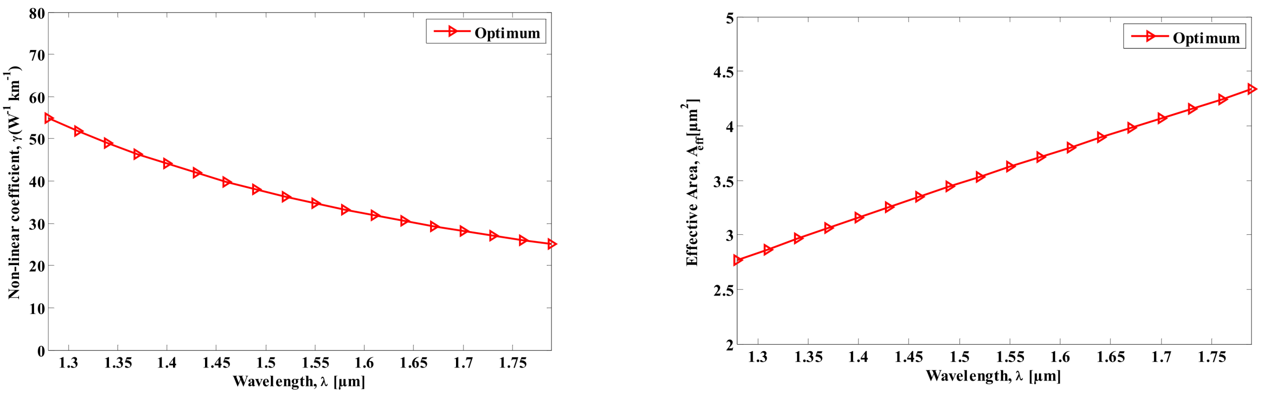

(**a**) (**b**)

Figure 6. The plot of wavelength dependent (**a**) nonlinear coefficient and (**b**) effective area of the proposed MHL-PCF at optimum design values.

Figure 7 illustrates the numerical aperture and confinement loss characteristics of the proposed MHL-PCF system at 1550 nm. At this wavelength, the numerical aperture value is predicted to be 0.4175, demonstrating the fiber's capacity to gather and receive light from a broad variety of angles. The figure also shows a confinement loss value of 0.114 dB/m, which represents the intensity of light retention within the fiber core. These findings shed light on the MHL-PCF's efficiency in directing and confining light at the prescribed wavelength, confirming its potential for use in optical communication and sensing systems.

Figure 8 depicts the distribution of the electric field for the fundamental mode at a wavelength of 1550 nm, illustrating both (a) the electric field distribution for x-polarization and (b) the electric field distribution for y-polarization. The modal properties of the proposed MHL-PCF were compared with the contemporary PCF designs in Table 1.

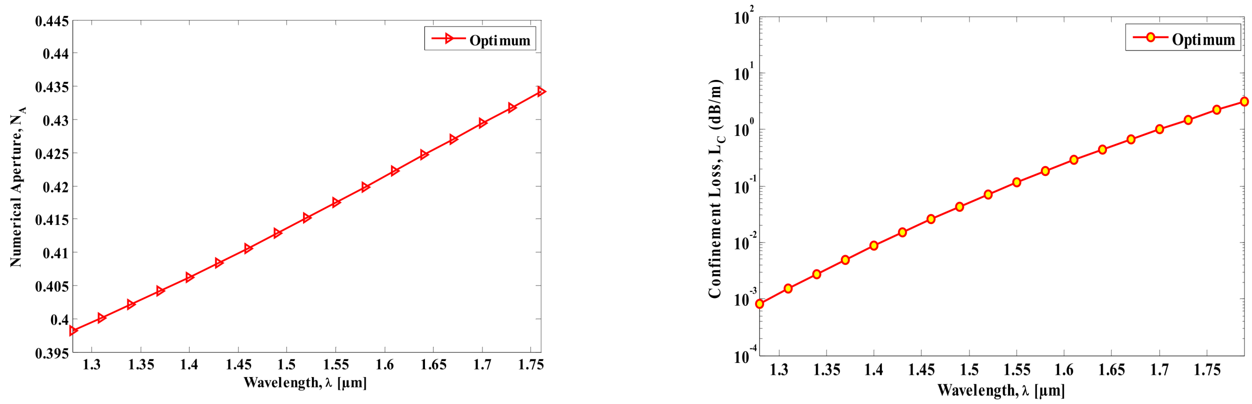

(**a**) (**b**)

Figure 7. Graphs illustrating the correlation between wavelength and numerical aperture (**a**), and wavelength and confinement loss (**b**), utilizing optimal geometric parameters of the proposed MHL-PCF design.

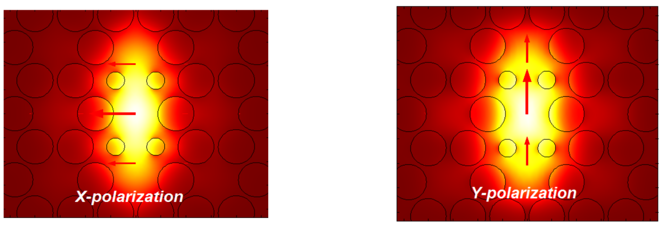

(**a**) (**b**)

Figure 8. The spatial distribution of the electric field for the fundamental mode at a wavelength of 1550 nm, showcasing (**a**) X-polarization and (**b**) Y-polarization.

Table 1. A concise comparison between existing Photonic Crystal Fiber (PCF) structures and the novel Modal Hybrid Lattice Photonic Crystal Fiber (MHL-PCF), specifically examining modal properties at a 1550 nm wavelength.

References	Dispersion, D [ps/(nm·km)]	Birefringence, B ($\times 10^{-2}$)	Nonlinear Coefficient, γ [$W^{-1}km^{-1}$]
[9]	−650	2.1	45.5
[10]	−578.5	2.64	53.1
[11]	−274.5	1.46	76.41
[12]	−11.63	--	--
[13]	−378.6	3.039	33.76
[14]	− 606	3.76	50.34
Proposed MHL-PCF	−652.9	1.482	34.68

5. Conclusions

In conclusion, this study offers a thorough investigation and design of a Broadband Dispersion Compensating Modified Honeycomb Lattice Photonic Crystal Fiber (MHL-PCF) with exceptional properties of high birefringence and nonlinearity. With a negative dispersion coefficient of −263.9 ps/(nm·km) at 1.55 µm and a high negative dispersion of −652.9 ps/(nm·km) throughout a tunable range of air-filled fraction, the proposed MHL-PCF displays remarkable dispersion compensation capabilities. Notably, the fiber's polarization-maintaining nature enhances its birefringence to 1.482×10^{-2} at the same operating frequency, complemented by a high nonlinear coefficient of 34.68 $W^{-1}km^{-1}$. The investigation of numerical aperture reveals excellent light-coupling properties, highlighting the fiber's potential for efficient light-guiding, dispersion control, and sensitivity in sensing applications. With its distinctive features, the suggested MHL-PCF emerges as a promising candidate for addressing the evolving demands of advanced optical communication systems, poised to facilitate high data rates over extended transmission distances through effective dispersion correction and nonlinear optical functionalities.

Author Contributions: Conceptualization, A.H.; methodology, A.H. and M.R.T.; software, A.H.; validation, M.A.H., M.S.A. and M.R.T.; formal analysis, A.H.; investigation, A.H.; resources, A.H. and M.S.A.; data curation, A.H.; writing—original draft preparation, A.H.; writing—review and editing, A.H. and M.S.A.; visualization, A.H.; supervision A.H.; project administration, M.R.T. and M.A.H. All authors have read and agreed to the published version of the manuscript.

Funding: This research received no external funding.

Institutional Review Board Statement: Not applicable.

Informed Consent Statement: Not applicable.

Data Availability Statement: The data presented in this study are available on request from the corresponding author.

Acknowledgments: The authors are grateful for the support from the Photonics Simulation Laboratory of the World University of Bangladesh, Dhaka-1230, Bangladesh.

Conflicts of Interest: The authors declare no conflict of interest.

References

1. Chi, N.; Zhou, Y.; Wei, Y.; Hu, F. Visible light communication in 6G: Advances, challenges, and prospects. *IEEE Veh. Technol. Mag.* **2020**, *15*, 93–102. [CrossRef]
2. Cvijetic, M.; Djordjevic, I. *Advanced Optical Communication Systems and Networks*; Artech House: Norwood, MA, USA, 2013.
3. Guo, X. *Controlling Light with Spatially and Temporally Phasemodulated Metasurfaces*; The Pennsylvania State University: State College, PA, USA, 2020.
4. Slusher, R.E. *Nonlinear Photonic Crystals*; Springer Science & Business Media: Berlin, Germany, 2003; Volume 10.
5. Garmire, E. Overview of nonlinear optics. In *Nonlinear Optics*; Intechopen: London, UK, 2012; pp. 3–52.
6. Bao, X.; Chen, L. Recent progress in distributed fiber optic sensors. *Sensors* **2012**, *12*, 8601–8639. [CrossRef]
7. Singh, S.; Singh, N. Nonlinear effects in optical fibers: Origin, management and applications. *Prog. Electromagn. Res.* **2007**, *73*, 249–275. [CrossRef]
8. Keiser, G.; Xiong, F.; Cui, Y.; Shum, P.P. Review of diverse optical fibers used in biomedical research and clinical practice. *J. Biomed. Opt.* **2014**, *19*, 080902. [CrossRef]
9. Haque, M.M.; Rahman, M.S.; Habib, M.S. A single mode hybrid cladding circular photonic crystal fiber dispersion compensation and sensing applications. *Photon- Nanostruct. Fundam. Appl.* **2015**, *14*, 63–70. [CrossRef]
10. Hasan, R.; Islam, A.; Rifat, A.A.; Hasan, I. A single-mode highly birefringent dispersion-compensating photonic crystal fiber using hybrid cladding. *J. Mod. Opt.* **2017**, *64*, 218–225. [CrossRef]
11. Prabu, K.; Malavika, R. Highly birefringent photonic crystal fiber with hybrid cladding. *Opt. Fiber Technol.* **2019**, *47*, 21–26. [CrossRef]
12. Krishna, G.D.; Pillai, V.M.; Gopchandran, K. Design of low dispersion and low loss photonic crystal fiber: Defected core circular-octagon hybrid lattices. *Opt. Fiber Technol.* **2019**, *51*, 17–24. [CrossRef]
13. Halder, A.; Anower, S. Relative dispersion slope matched highly birefringent and highly nonlinear dispersion compensating hybrid photonic crystal fiber. *Photon- Nanostruct. Fundam. Appl.* **2019**, *35*, 100704. [CrossRef]
14. Halder, A. Slope matched highly birefringent hybrid dispersion compensating fiber over telecommunication bands with low confinement loss. *J. Opt.* **2020**, *49*, 187–195. [CrossRef]
15. Bise, R.T.; Trevor, D.J. Sol-Gel Derived Microstructured Fiber: Fabrication and Characterization. In *Optical Fiber Communication Conference*; Optica Publishing Group: Washington, DC, USA, 2005; p. OWL6.
16. Zhang, P.; Zhang, J.; Yang, P.; Dai, S.; Wang, X.; Zhang, W. Fabrication of chalcogenide glass photonic crystal fibers with mechanical drilling. *Opt. Fiber Technol.* **2015**, *26*, 176–179. [CrossRef]
17. Chow, D.M.; Sandoghchi, S.R.; Adikan, F.M. Fabrication of photonic crystal fibers. In Proceedings of the 2012 IEEE 3rd International Conference on Photonics, Pulau Pinang, Malaysia, 1–3 October 2012; IEEE: Piscataway, NJ, USA, 2012; pp. 227–230.
18. Jagota, V.; Sethi, A.P.S.; Kumar, K. Finite element method: An overview. *Walailak J. Sci. Technol. (WJST)* **2013**, *10*, 1–8.
19. Khalek, A.; Chakma, S.; Paul, B.K.; Ahmed, K. Dataset of surface plasmon resonance based on photonic crystal fiber for chemical sensing applications. *Data Brief* **2018**, *19*, 76–81. [CrossRef] [PubMed]
20. Prabesh, D. Development and Characterization of Novel Garnet and Gold Thin Films for Photonic and Plasmonic Applications. Ph.D. Thesis, University of Minnesota, Minneapolis, MN, USA, 2017.

21. Brückner, V. To the use of Sellmeier formula. *Sr. Expert. Serv. (SES) Bonn HfT Leipz. Ger.* **2011**, *42*, 242–250.
22. Shao-Wen, G.; Jun-Cheng, C.; Song-Lin, F. Numerical Analysis of Multilayer Waveguides Using Effective Refractive Index Method. *Commun. Theor. Phys.* **2003**, *39*, 327–330. [CrossRef]
23. Moughli, H.; Mouloudi, Y.; Merabti, A. Study and modeling of photonic crystal fibers. *J. Ovonic Res.* **2022**, *18*, 491–497. [CrossRef]
24. Bachim, B.L.; Gaylord, T.K. Polarization-dependent loss and birefringence in long-period fiber gratings. *Appl. Opt.* **2003**, *42*, 6816–6823. [CrossRef]
25. Koshiba, M.; Saitoh, K. Structural dependence of effective area and mode field diameter for holey fibers. *Opt. Express* **2003**, *11*, 1746–1756. [CrossRef]
26. Razzak, S.M.A.; Namihira, Y. Proposal for Highly Nonlinear Dispersion-Flattened Octagonal Photonic Crystal Fibers. *IEEE Photon- Technol. Lett.* **2008**, *20*, 249–251. [CrossRef]
27. Matsui, T.; Zhou, J.; Nakajima, K.; Sankawa, I. Dispersion-flattened photonic crystal fiber with large effective area and low confinement loss. *J. Light. Technol.* **2005**, *23*, 4178–4183. [CrossRef]
28. Mortensen, N.; Folken, J.; Skovgaard, P.; Broeng, J. Numerical aperture of single-mode photonic crystal fibers. *IEEE Photon-Technol. Lett.* **2002**, *14*, 1094–1096. [CrossRef]
29. Dudley, J.M.; Taylor, J.R. (Eds.) *Supercontinuum Generation in Optical Fibers*; Cambridge University Press: Cambridge, UK, 2010.